

Theoretical Investigation of the Gas-Phase Kinetics Active during the GaN MOVPE

Davide Moscatelli and Carlo Cavallotti*

Dept. di Chimica, Materiali e Ingegneria Chimica "G. Natta", Politecnico di Milano,
Via Mancinelli 7 – 20131 Milano, Italy

Received: December 4, 2006; In Final Form: February 9, 2007

Quantum chemistry investigations have been performed to study the gas-phase chemistry active during the MOVPE of GaN when $\text{Ga}(\text{CH}_3)_3$ and NH_3 , diluted in a H_2 carrier gas, are used as precursors. Optimized molecular geometries, energies, and transition-state structures of gas-phase species have been determined with density functional theory at the B3LYP/6-311+g(d,p) level. On the basis of the similarity with the soot formation mechanism active during hydrocarbon combustion, we propose that in this system a gas-phase chemistry is active and its reactivity is enhanced by a radical chain mechanism started from methyl radicals. Initiation reactions are surface processes or the pyrolysis of $\text{Ga}(\text{CH}_3)_3$. A propagation mechanism composed of fast radical reactions, most of which without an activation energy, was identified, and kinetic constants were determined for each step. The proposed mechanism is able to describe the formation of large GaN adducts formed by up to three R–Ga–NH units. These molecules can give fast cyclization reactions that lead to the formation of six-membered cyclic species, which, similar to benzene for combustion, are thermodynamically stable in vast temperature and pressure ranges and can thus be considered as the first GaN nuclei. We also found that the presence of H_2 as a carrier gas can greatly enhance the rate of formation of gas-phase particles because it is a major source of atomic hydrogen, a promoter of gas-phase reactivity.

1. Introduction

Gallium nitride (GaN) attracts great interest because of its several applications in optoelectronic, high-power, and high-frequency devices. It is a binary III/V direct wide band gap semiconductor (3.4 eV), and it is considered by many as the most important semiconductor material after silicon. It can be used to produce brilliant blue light and is among the most promising materials for the next generation of high-temperature transistors.^{1,2} Moreover, gallium nitride is the semiconductor compound expected to make miniaturized, high-power wireless transmitters possible, which might be joined to sensitive receivers into telephone sets capable of accessing communication satellites directly.³ The advantages of GaN devices include high output power with small physical volume⁴ and high efficiency in power amplifiers at ultrahigh and microwave radio frequencies.^{1,2,5}

The preferred industrial method of producing gallium nitride is metal organic vapor-phase epitaxy (MOVPE). The deposition of GaN is conducted typically at temperatures of 1000 °C, usually adopting ammonia and trimethylgallium (TMGa) as reactants with a V–III ratio (NH_3/TMGa) higher than 1000, and hydrogen as the carrier gas.^{5,6} Major problems encountered during the growth of high-quality films are represented both by the absence of a homoepitaxial substrate, so that films are usually deposited on sapphire, which has a lattice mismatch of 14% with GaN, and by the presence of severe parasitic gas-phase reactions. These undesired reactions lead to the formation of GaN gas-phase adducts and thus determine the nucleation of particles formed by several gallium, nitrogen, carbon, and hydrogen atoms.^{7–11} Once generated, GaN powders can adsorb on the reactor walls or the growth surface, thus affecting the film

quality, though this process is contrasted by thermal diffusion, which hinders the diffusion of heavy particles toward hot surfaces if a sufficient thermal gradient is present. The formation of gas-phase particles is an important technological problem because it is associated with the following: loss of precursors, which will not be available for deposition; fouling of the reactor, which must therefore be cleaned periodically; formation of stable intermediate species of relatively low molecular weight, thus only slightly affected by thermal diffusion, which might adsorb on the surface in positions that might not be epitaxial and thus give rise to the formation of defects, such as stacking faults.⁶

In this framework, the aim of the present investigation is the development of a gas-phase kinetic scheme apt to explain the mechanism of formation of GaN powders, along with the identification of the main precursors to the deposition of GaN.

Experimental observations have shown that at low reaction temperatures (400–500 K) the gas-phase reactivity of GaN proceeds through the formation of donor–acceptor complexes (i.e., $\text{Ga}(\text{CH}_3)_3:\text{NH}_3$) due to the electron deficiency of alkyl–gallium compounds and the basic properties of ammonia.^{8,12} This experimental evidence is supported by theoretical results that also revealed how the formation of these acid–base adducts is exothermic by about 16 kcal/mol.^{13,14} Along the formation of these complexes, the production of methane and gallium–nitrogen adducts, which we refer to as amides (i.e., $\text{Ga}(\text{CH}_3)_2\text{-NH}_2$), has been detected. This chemical pathway, known as the “amide mechanism” and in which adduct condensation reactions play a major role, represents a first possible mechanism of formation of molecules with a Ga–N bond.⁸ It was also found that $\text{Ga}(\text{CH}_3)_2\text{NH}_2$ can be isolated in a trimeric form: $[\text{Ga}(\text{CH}_3)_2\text{NH}_2]_3$. The possibility that this compound is involved in the GaN nanoparticle formation has been advanced^{10,15} and disputed.^{4,6,8,16} To complete the GaN gas-phase condensation scenario, it is useful to mention the extensive theoretical study

* Author to whom correspondence should be addressed. E-mail: carlo.cavallotti@polimi.it. Tel: ++39-02-23993176. Fax: ++39-02-23993180.

made by Mihopoulos for the MOVPE of AlGaIn, who investigated several possible high-temperature condensation reactions that produce GaN or AlN molecules and methane.¹⁰

Although at room-temperature chemical pathways active in the GaN gas phase are dominated by reversible formation and dissociation of acid–base adducts without methane detection, the increase of the reaction temperature leads to the activation of a huge number of reactions, most of which are not yet well understood.^{4,8,17,18} Experimental results have shown that the products of these reactions are gas-phase molecules characterized by gallium–nitrogen bonds. However, it is difficult to clearly identify the exact structure of these compounds.

Given the complexity of developing a reliable gas-phase diagnostic designed for the GaN MOVPE, the gas-phase chemistry of GaN has been investigated more in detail through theoretical approaches. In several computational investigations, Timoshkin has determined structures, energies, and frequencies of a great number of possible high molecular weight gas-phase molecules. Thermodynamically favorite geometries of these compounds are represented by tetracoordinate dimers, trimers, tetramers, and hexamers that can assume a large number of potential stable configurations, among which many are cyclic or cubic.^{4,13,14}

Although not much is known on the GaN gas-phase reactivity, much work has been devoted to the study of the decomposition mechanism of the most important gas-phase gallium precursor: Ga(CH₃)₃. At high temperature, the pyrolysis of Ga(CH₃)₃ proceeds at a significant rate through the successive homolysis of gallium–carbon bonds. The measured rate constant of this reaction is $3.16 \times 10^{15} \exp(59.48/RT)$.¹⁹ Along this experimental evidence, different theoretical investigations have been made in order to elucidate the kinetics of this process. The Arrhenius parameters for the first Ga–C bond homolysis of TMGa have been estimated computationally by Schmid using density functional theory and coupled-cluster calculations.⁶ This study showed that the activation energy for the Ga(CH₃)₃ dissociation is probably 7 kcal/mol higher than that measured experimentally and that the underestimation is likely to be due to an enhanced surface reactivity that increases the Ga(CH₃)₃ dissociation rate. In any case, both experimental and theoretical studies agree that, at temperatures higher than 700 °C, Ga(CH₃)₃ decomposes to Ga(CH₃) and two methyl radicals. On the basis of this and other experimental observations, some authors have proposed that the GaN gas-phase reactivity is significantly influenced by radical reactions, though no specific indication of the nature and rate of such reactions have been proposed.^{8,16,20}

The mechanism we propose here to explain the gas-phase reactivity of GaN differs from those based on neutral–neutral reactions proceeding through methane elimination and is based on the hypothesis that the formation of GaN powders in the gas phase follows a reaction mechanism similar to that used in hydrocarbon combustion chemistry to describe soot formation.^{21–23} This hypothesis is based on our previous theoretical studies in which we have shown that gas-phase reactions active during the MOVPE of several semiconductor materials such as ZnSe, ZnS, CdTe, GaAs, AlAs, AlGaAs, and InP are strongly enhanced by the presence of radicals that are generated at the surface, in particular when hydrogen is used as the carrier gas.^{24–30} This can lead to a radical chain of reactions that can eventually end in the formation of gas-phase adducts. Concerning the MOVPE of GaN, radicals can be produced both as a result of surface reactivity and through pyrolysis reactions. After the formation of gas-phase adducts, it is possible, as in the case

of soot nucleation in combustion, that these molecules coagulate producing GaN particles.²¹

Our theoretical approach is based on the use of density functional theory (DFT), which combines good accuracy with limited computational demand, to determine thermodynamic parameters and structures of reactants, products, and transition states. Rate constants for reactions that require overcoming an activation energy have been determined with transition-state theory (TST), whereas the rate of barrierless reaction was calculated with the gas kinetic theory.

2. Computational Details. Gas-phase reactions involved in the metal organic vapor-phase epitaxy (MOVPE) of GaN were investigated by combining density functional theory calculations with a suitable kinetic theory. In particular, in all of the DFT calculations the Becke 3 parameters and Lee Yang Parr functionals were adopted to evaluate the exchange and correlation energy.^{31,32} This computational method has already given good results in the study of similar reacting systems.^{4,16,28,29} The triple- ζ all-electron 6-311 basis set with added polarization and diffuse functions (6-311+g(d,p))³³ was used in the calculations because it allows us to determine the structures and energies of the gallium–nitrogen system with reasonable accuracy.⁶ As a general rule, all geometries were fully optimized with the Berny algorithm and were followed by frequency calculations.^{34,35} Because it is known that vibrational frequencies smaller than 150 cm⁻¹ can degenerate into rotational motions, we considered explicitly low frequencies as rotors or hindered rotors when found necessary.

The geometry of each molecular structure was considered stable only after calculating vibrational frequencies and force constants and if no imaginary vibrational frequency was found. Transition-state structures were located by adopting the synchronous transit-guided quasi-Newton method and were characterized by a single imaginary vibrational frequency.³⁵ Kinetic constants were estimated with conventional transition-state theory if a distinct transition state could be identified. Otherwise, for reactions proceeding without overcoming an energetic maximum on the PES, kinetic constants were calculated by adopting collisional theory as

$$k^{\text{coll}} = \chi \left(\frac{d_A + d_B}{2} \right)^2 \frac{N_A^2}{10^6} \sqrt{8\pi k_b T \left(\frac{1}{M_A} + \frac{1}{M_B} \right)} \quad (1)$$

where d_i , M_i , and N_i are the collisional diameter, the molecular weight, and the Avogadro constant. χ is a steric factor that is between 0 and 1 and represents the collisional efficiency. As discussed in detail in our work on the MOVPE of GaAs and AlAs,³⁶ the collisional diameter for atomic species was assumed to be equal to the covalent radius and χ was set to one. For other molecular species, the collisional diameter is considered equal to half of the sum of the forming bond length with the van der Waals radius of the involved atoms. χ cannot be estimated easily in this case; thus, we approximated its value to the product of the Van der Waals active surfaces of the two involved reactants. Calculated χ values are always less than 1; as an example, for reaction 48 the active surface area ratio of the radical GaNH• is 0.5 because only the half-radical part of the molecule participates actively to the reactive process. The same value was determined for the Ga(CH₃) species leading to a steric factor for the reaction between Ga(CH₃) and GaNH• of 0.25. The parameters adopted to estimate the collisional rate are reported in Table 1.

Kinetic constant pressure dependence and internal energy transfer was not investigated in this work. All kinetic constants

TABLE 1: Parameters Adopted to Estimate Collisional Kinetic Constants (Values Are Reported in Angstroms)

atom	radius	fragment	bond length
H	0.32	Ga—C	1.99
Ga	1.26	Ga—H	1.55
C	0.77	Ga—N	1.83
N	0.75	C—H	1.09
		N—H	1.01

reactive species	fragment diameter (range)
CH ₃ •, NH ₂ •	1.5–2.5
Ga(CH ₃) ₃ , Ga(NH ₂) ₃ , GaNH•, Ga(μ2 - NH)Ga	2.5–3.5
Ga(CH ₃) _x (NH ₂) _{1-x} , Ga(CH ₃) _x (NH ₂) _{2-x} NH•,	3.5–6.0
Ga(μ2 - NH)Ga(CH ₃) _x , Ga ₂ N ₂ , Ga ₂ NNH•	
Ga(CH ₃) _x (NH ₂) _{1-x} , Ga(CH ₃) _x (NH ₂) _{2-x} NH•,	4.0–7.5
Ga(μ2 - NH)Ga(CH ₃) _x , Ga ₂ (CH ₃) _x (NH) ₂ , Ga ₂ (CH ₃) _x (NH)NH•	
Ga ₃ (CH ₃) _x (NH) ₂ , Ga ₃ (CH ₃) _x (NH)NH•, Ga ₃ (CH ₃) _x (NH) ₃ ,	6.5–11.0
Ga ₃ (CH ₃) _x (NH) ₂ NH•, Ga ₃ N ₃ cyclic	

reported here are thus to be considered in their high-pressure limit. However, because most of the reactions considered are bimolecular processes proceeding without the formation of a vibrationally excited intermediate state, it is likely that their kinetic constant will be pressure-independent. The only exceptions are unimolecular cyclization reactions discussed in paragraph 3.3.3.

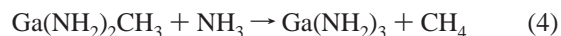
All quantum chemistry calculations were performed with the Gaussian 03 suite of programs,³⁷ and all pictures were drawn with Molden 4.2.³⁸

3. Results and Discussion

This work was organized as follows. First, we tested our computational approach by determining the kinetic constants of the condensation reactions and comparing obtained results with those reported in literature. After that, we defined on a thermodynamic background the field of our investigation in order to limit the number of chemical species to be considered. Then we calculated the kinetic constants of key reactions involved in the production of the first reactive radical species. After being generated, these radicals react with other gas-phase molecules starting a radical chain mechanism. Thus, we successively identified three consecutive catalytic cycles that eventually lead to the formation of GaN gas-phase adducts containing up to three R–Ga–NH units. The calculated thermodynamic parameters and kinetic constants are collected in tables and organized so that they can be inserted in a kinetic mechanism and reactor model promptly.

3.1. Gas-Phase Reactivity: Condensation Reactions and Definition of Investigated Field. In the first part of this work, we studied high-temperature condensation reactions. Because

these reactions have already been well investigated in the literature, these calculations were aimed both at estimating the accuracy of our computational procedure and at determining the rate of some reactions for which kinetic parameters were not available.¹⁶ The condensation mechanism involves the direct reaction between the precursors to give Ga(CH₃)₂NH₂ and CH₄ followed by consecutive addition of ammonia and elimination of methane. The first reactions studied were the following:



The PES of reaction 2, reported in Figure 1a, confirms the trend reported in the literature:^{6,16} the formation of a donor–acceptor complex characterized by an enthalpy change at 298 K of 15.68 kcal/mol, followed by the evolution to the products passing through a transition state. The rate of this class of reactions can be calculated at high pressures either assuming that adduct and reactants are in chemical equilibrium, and then determining the reaction rate as that of a unimolecular process using conventional transition state theory, or neglecting the formation of the adduct, which is reasonable if the adduct binding energy is small and temperatures are high, and calculating the reaction rate as that of a bimolecular process. For this particular case, we choose the second option, given the small stabilization energy of the adduct (about 15 kcal/mol) and the high temperature at which the GaN MOVPE is performed (~1000 °C). All three reactions are exothermic by about

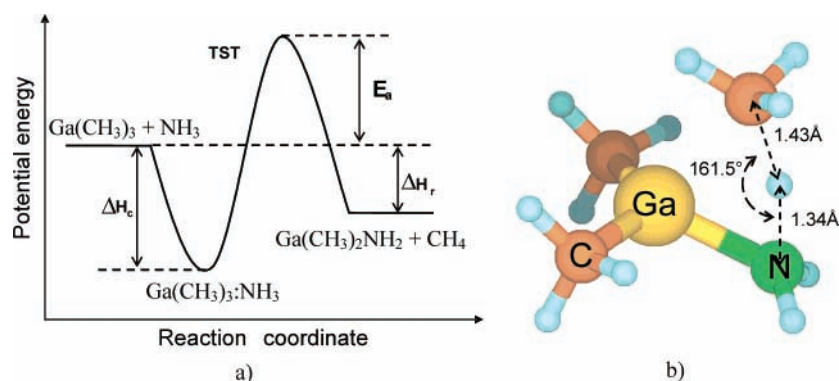


Figure 1. (a) potential energy surface of reaction 2; ΔH_c , E_a , and ΔH_r represent the enthalpy change of donor–acceptor complex formation, the reaction activation energy, and the reaction enthalpy change, respectively. (b) Transition-state structure for the condensation reaction between Ga(CH₃)₃ and NH₃.

TABLE 2: Kinetic Constants of Condensation Reactions^a

	reaction	$\log_{10} A$	α	E_a	ΔH_r
2	$\text{Ga}(\text{CH}_3)_3 + \text{NH}_3 \rightarrow \text{Ga}(\text{CH}_3)_2\text{NH}_2 + \text{CH}_4$	7.544	1.0	17.93	-18.89
3	$\text{Ga}(\text{CH}_3)_2\text{NH}_2 + \text{NH}_3 \rightarrow \text{Ga}(\text{NH}_2)_2\text{CH}_3 + \text{CH}_4$	7.328	1.0	18.00	-14.11
4	$\text{Ga}(\text{NH}_2)_2\text{CH}_3 + \text{NH}_3 \rightarrow \text{Ga}(\text{NH}_2)_3 + \text{CH}_4$	7.211	1.0	18.22	-9.82
5	$\text{Ga}(\text{CH}_3) + \text{NH}_3 \rightarrow \text{Ga}(\text{NH}_2) + \text{CH}_4$	9.332	1.0	18.50	-23.92
6	$\text{Ga}(\text{NH}_2) + \text{Ga}(\text{CH}_3) \rightarrow \text{Ga}(\mu 2 - \text{NH})\text{Ga} + \text{CH}_4$	9.510	1.0	16.40	-26.44

^a Reaction rate coefficients expressed as $k = AT^\alpha \exp(-E_a/RT)$; data consistent with units in kcal, mol, cm, s. Reaction enthalpies are calculated at 298 K.

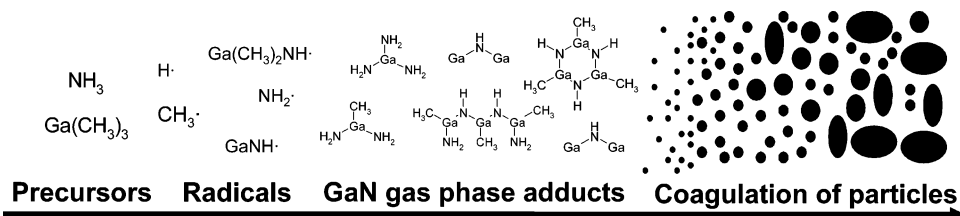


Figure 2. GaN gas-phase nuclei formation scheme adapted from the scheme proposed by Bockhorn to describe the soot formation in hydrocarbon flames.²¹

20 kcal/mol and have activation energies between 17.9 and 20.0 kcal/mol. The kinetic constants have similar pre-exponential factors of about $3.5 \times 10^7 T$ (K). For reaction 2, the transition-state structure is reported in Figure 1b.

Along with reactions 2–4, we determined other possible condensation reactions starting from small GaN gas-phase compounds to give methane and increasingly complicated GaN species. Also in this case, these reactions require overcoming a relatively small activation energy, which is, however, likely to decrease substantially the reaction rate at the considered temperatures. The calculated rate-constant parameters for these reactions are reported in Table 2.

Results reported in the literature show that reaction 2 has an activation energy of about 19 kcal/mol,¹⁶ in agreement with those determined in this work. However, a comparison with kinetic constants involved in the MOVPE processes of other semiconductor compounds, in which previously theoretical investigations demonstrate the importance of radical reactions (for example, ZnSe, CdTe, AlGaAs), shows how the calculated condensation reaction rates are slower than those characteristic of a radical pathway.^{24,30,36} In fact, MOVPE radical reactions generally have no activation energy (or, in any studied case, smaller than 5–10 kcal/mol) and pre-exponential factors 1–2 orders of magnitude higher than those of reactions 2–6. In this framework, it is interesting to evaluate, using the computed condensation kinetic constants, the residence time in a perfectly stirred reactor necessary to obtain a significant formation of GaN adducts in the gas phase. This can be determined in first approximation as

$$\tau = \frac{C_{\text{nuclei}}^{\text{out}}}{k_R \prod C_{\text{reactants}}^{\text{in}}} = \frac{RT}{P} \frac{X_{\text{nuclei}}^{\text{out}}}{K_R \prod X_{\text{reactants}}^{\text{in}}} \quad (7)$$

where k_R is the kinetic constant of the condensation reaction that produces the adduct, T and P are temperature and pressure, R is the gas constant, C_i is the concentration of the i th chemical species, and X_i is its mole fraction.¹ Typical operating conditions of reactors adopted to deposit GaN film are the following: pressures of 50 Torr, temperatures higher than 1000 °C, and inlet mole fractions of V and III precursors of about 10^{-3} and 0.5, respectively. In such conditions, the residence time necessary to obtain through a condensation mechanism the formation of a significant amount of gas-phase adducts (i.e., 10^{-6}) is 10 s, which is much higher than the usual residence times in

CVD reactors (about 10^{-1} s). This suggests that the condensation rate at which the reaction between the precursors proceed is too small to justify the formation of adducts. Thus, a radical chain mechanism could represent an alternative reaction pathway, provided that radicals are produced in a consistent amount during the growth process.

At typical temperatures of deposition of GaN (greater than 1000 °C), it is known that for both II–VI and III–V compounds a significant amount of radical species are desorbed from the growing surfaces during the growth process. The exact nature of the desorbed hydrocarbon radicals depends on the precursors adopted. These radicals may lead to the formation of a high number of different GaN gas-phase adducts, which might be considered as precursors to stable nuclei, as reported schematically in Figure 2.

The mechanism of powder formation we propose and investigate here is analogous to that proposed to explain the formation of soot during the combustion of hydrocarbons. Because it is known that soot formation mechanisms can be extremely complex, comprising hundreds of chemical species involved in thousands of reactions,³⁹ we decided to limit the investigated reaction field imposing some approximations.

First, we calculated the energies and entropies of many possible molecules formed by Ga and a combination of N, H, and C (some of these compounds have already been studied in the literature^{4,13,14}). We did not consider unsaturated species because of the low probability of a gallium atom to form a π bond with either N or C (in any case this would be a very weak bond). For the same reason, we did not take into account species with Ga–Ga bonds. Hydrocarbons characterized by the formation of more than one C–C bond and Ga compounds in which N–N and C–N bonds are present have not been considered. This choice has been made because methane is the most thermodynamically stable hydrocarbon in the temperature ranges considered, while the energy of N–N and C–N bonds is smaller than that of the respective N–H and C–H bonds. This suggests that the formation of such compounds, though some are thermodynamically stable, such as HCN, is likely to be hindered by kinetic barriers. As a result of this preliminary study, the investigation has been focused on gas-phase species composed of gallium atoms with valence equal to 1 or 3 (Ga compounds with valence 2 are unstable²⁶) bonded with methyl, an amino group, or an amino group partially substituted with other gallium atoms (e.g., $\text{Ga}(\mu 2 - \text{NH})\text{Ga}$).

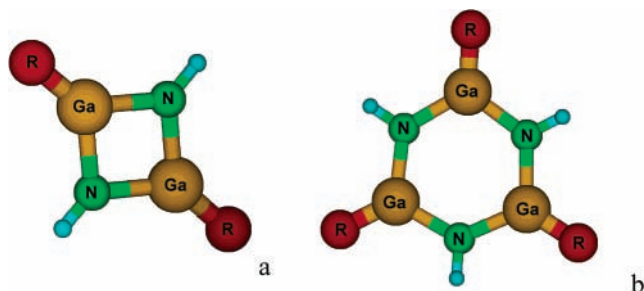


Figure 3. General structure of (a) a four-membered ring and (b) a six-membered ring. R represents a CH₃, H, or NH₂ group.

A second approximation of fundamental importance in order to limit the field of investigation is the definition of the maximum size of the considered GaN molecules. This represents an upper limit to the total number of reactions and chemical species that must be considered in the chemical mechanism. Similar to what is often done in combustion, we choose to limit the extent of our study to the formation of the first thermodynamically stable GaN nuclei. The reason for this choice is that a chemical species which is thermodynamically stable with respect to reactants will have, as the only possible reaction possibility, that of being converted to a more stable, and generally larger, chemical species. This is the reason that powder growth models, such as the momentum method, require as input the rate of formation of the smallest thermodynamically stable nuclei, which is often a very difficult parameter to determine.⁴⁰ In this framework, the advantage of our kinetic mechanism is that, when inserted in a suitable fluid dynamic model, it will predict the rate of GaN nuclei formation as a function of the reactor geometry and operating conditions.

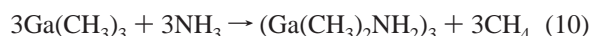
As reported previously, recent computational investigations performed by Timoshkin et al. have identified some stable structures of possible donor–acceptor complexes of GaN.^{4,13,14} These works show how reactants molecules can be arranged in complex structures such as cubic tetramers and hexamers, and, more in general, that the formation of GaN cyclic oligomers is usually energetically favored. The smallest oligomers considered were dimers and trimers so that we first studied whether cyclic GaN molecules containing two or three GaN units were stable with respect to precursors. In particular, we considered the following cyclization reactions:



The structures of the (R–Ga–NH)_x oligomers are sketched in Figure 3. The calculated free-energy changes for reactions 8 and 9 are 34.32 and –12.97 kcal/mol at 1000 °C. These results clearly indicate that the formation of a six-membered cyclic species is significantly more favored than that of a four-membered species. The reason is that both Ga and N can form stable tricoordinated species with bond angles of about 120°. The formation of a four- with respect to a six-membered cyclic species is therefore unfavored both from an energetic standpoint, because the four ring is more strained than the six ring, and from an entropic point of view. In fact, the entropy change for reaction 9 is significantly larger than that of reaction 8, mainly because the number of chemical species increases by one unit in 9, whereas in 8 it remains the same (for reaction 8 the enthalpy change is 20.99 kcal/mol and the entropy change –10.48 cal/mol/K, whereas for reaction 9 energetic and entropic changes are –5.87 kcal/mol and 5.57 cal/mol/K, respectively).

On the basis of these considerations, we therefore chose a (R–Ga–NH)₃ trimer where R could be CH₃, NH₂, or H, as representative of the first stable nuclei that can be formed in a GaN atmosphere. It is interesting that this species remembers, for the chemical structure, the molecule considered in combustion as the first precursor to soot formation: benzene.

We would finally like to observe that the (R–Ga–NH)₃ trimer differs from the GaN adduct that has been initially proposed as precursor to the formation of GaN powders: (Ga–(CH₃)₂NH₂)₃.^{15,41} The possibility that this molecule might form during GaN MOVPE has in fact been questioned recently on a kinetic basis.¹⁶ Moreover, by applying the same thermodynamic considerations, we can observe that the free-energy change for the formation of (Ga(CH₃)₂NH₂)₃ at 1000 °C is 151.64 kcal/mol. This, which indicates that this species is thermodynamically unstable with respect to the reactants, can be explained considering its formation reaction:



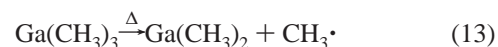
As can be observed this reaction, characterized by a decrease of the total number of chemical species of –2, is entropically (ΔS at 1000 °C is –115.01 cal/mol/K) and energetically (ΔH at 1000 °C is 5.23 kcal/mol/K) extremely unfavored.

3.2. Radical Generation Mechanism and First Propagation Reactions. Many experimental and theoretical studies have been performed in order to better understand the fundamental reactions that take place during the MOVPE of Ga-based semiconductors. Results of these researches have clarified how the metal organic precursors of gallium, in particular TMGa, react with the growing surface atoms producing free hydrocarbon radicals. The growth proceeds through the dissociative adsorption of TMGa to give a Ga(CH₃) species adsorbed over the growing surface, followed by methyl desorption.^{42–46} Another important growth precursor is Ga(CH₃), which is present in the gas phase as a result of the thermal decomposition of TMGa. The TMGa and MMGa adsorption reactions proceed through the following global stoichiometry:



The dissociation of the methyl group from GaCH₃* species is an activated process that requires about 49 kcal/mol.^{44,46} After being generated by surface reactions, methyl radicals can then diffuse rapidly in the gas phase.

In addition, methyl radicals, as widely reported in literature,^{6,7,16} can also be produced directly in the gas phase as a result of thermal decomposition of both TMGa and adducts produced through gas-phase reactions as



The Ga(CH₃)₂ species (or equivalent gas phase-adducts characterized by a gallium atom with valence 2, as the product of reaction 14) is quite unstable and, as reported in previous works,^{26,36} it spontaneously expels a methyl radical to form the more stable monomethylgallium (MMGa) molecule through the following reaction:

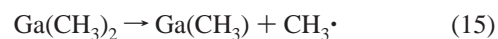


TABLE 3: Rate Coefficients of Reactions Started from Methyl Radicals, Expressed as $k = AT^\alpha \exp(-Ea/RT)$ and Consistent with Units in kcal, mol, cm, s

reaction	$\log_{10}A$	α	Ea	ref
16 $\text{CH}_3\cdot + \text{NH}_3 \leftrightarrow \text{CH}_4 + \text{NH}_2\cdot$	3.40	2.86	14.6	48
reverse	1.49	3.59	9.02	49
17 $\text{CH}_3\cdot + \text{H}_2 \leftrightarrow \text{CH}_4 + \text{H}\cdot$	3.81	2.70	8.86	50
reverse	3.60	3.16	8.75	51
18 $\text{H}\cdot + \text{NH}_3 \leftrightarrow \text{H}_2 + \text{NH}_2\cdot$	4.76	2.76	10.27	52
reverse	3.20	2.83	7.23	52

The nature of this instability is due to the external electronic configuration of the gallium atom, which forms preferentially either three covalent bonds (involving in this case all of its external electrons) or one covalent bond (leaving coupled two external electrons).

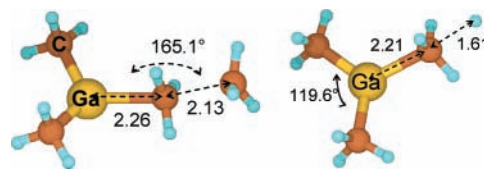
The calculated activation energy for reactions 13 and 14 is 68.9 kcal/mol, in agreement with the CCSD(T)/cc-pvdz computational results of Schmid, who reports a value of 71.1 (corrected for BSSE, uncorrected for ZPE, which is -4.4 kcal/mol at the B3LYP/6-311+g(d,p) level).⁶ The small difference of 2.3 kcal/mol between $(\text{CH}_3)_2\text{Ga}-\text{CH}_3$ bond energies calculated at the coupled-cluster and DFT levels indicates that the computational approach adopted here describes Ga-alkyl bonds reasonably well. The experimental activation energy for this kinetic step (59.48 ± 5.5 kcal/mol)¹⁹ is smaller, which might be due to an experimental overestimation of the decomposition rate determined by a surface catalytic effect.⁴⁷

To determine the relative error of B3LYP/6-311+g(d,p) calculations with respect to higher level theories, we calculated the Ga-NH₂ and Ga-CH₃ bond energies at the CCSD(T)/cc-pvtz level, on structures optimized at the B3LYP/6-311+g(d,p) level. The DFT binding energies differ from CCSD values by less than 2 kcal/mol in both cases, thus confirming the reliability of the approach adopted here.

Concerning the rupture of the second gallium-carbon bond and the relative production of a free methyl radical, we calculated an activation energy of 28.3 kcal/mol. Also in this case the value is in agreement with the experimental data (35.4 kcal/mol).¹⁹ It is then possible to conclude that both the gas-phase homogeneous pyrolysis of the precursor and the dissociative adsorption of gallium species over the surface lead to the formation of reactive methyl radicals.⁸

After being generated as result of both gas-phase pyrolysis of TMGa and film growth, methyl radicals can react with the most abundant chemical species present in the gas phase. Because of the reactive nature of $\text{CH}_3\cdot$ and the high temperature adopted in the GaN MOVPE, the carrier gases (hydrogen + NH_3) are likely to influence the chemistry of this system significantly. Thus, the first reactions considered were those between $\text{CH}_3\cdot$, H_2 , and NH_3 . For these reactions, forward and backward kinetic constants are available in the literature and are summarized in Table 3. Hydrogen, ammonia, and methyl radicals are characterized by a high reactivity and can then react with the Ga precursors. Here it is important to observe that the methyl radical reacts much faster with H_2 than NH_3 . At 1000 °C, the rate of reaction 17, at parity of H_2 and NH_3 concentration, is in fact 8 times higher than that of reaction 16. Atomic hydrogen, once produced through reaction 17, can then react with NH_3 to form $\text{NH}_2\cdot$ at a rate that is about 2 orders of magnitude higher than that of reaction 16. We can thus conclude that one of the effects of using H_2 as a carrier gas is that of increasing the $\text{NH}_2\cdot$ and $\text{H}\cdot$ radical concentration. We will discuss later how this is related to the GaN nucleation rate.

3.3. Radical Chain Mechanism. In this section, we investigate possible radical chain mechanisms that can lead to the

**Figure 4.** Transition-state structure for reactions 19 (left) and 20 (right). Distances are reported in angstroms, and angles are reported in degrees.

formation of thermodynamically stable nuclei. Despite the large number of reactions considered, we do not intend for this investigation to be exhaustive of all of the possible reaction pathways but rather a study focused on at least one fast radical mechanism that can lead to the formation of powders in GaN atmospheres.

3.3.1. First Catalytic Cycle. The first reactions involved in the catalytic cycle are those between the gas-phase precursor, $\text{Ga}(\text{CH}_3)_3$, methyl radicals produced by the pyrolysis of TMGa or as a consequence of the film growth, and $\text{H}\cdot$ and $\text{NH}_2\cdot$ radicals formed in reactions 16–18. In particular, the first reactions considered involve the gas-phase radicals produced in the initiation reactions and the Ga precursors.

The products of reactions 19 and 20, the transition-state structures of which are reported in Figure 4, are $\text{Ga}(\text{CH}_3)_2$, which further dissociates to give MMGa and a methyl radical, and an alkane molecule (methane or ethane, respectively). Because $\text{Ga}(\text{CH}_3)_2$ is unstable with respect to $\text{Ga}(\text{CH}_3)$ and CH_3 , we directly report the products of its dissociation. The calculated rate constant and enthalpy changes are summarized in Table 4. In general, it can be observed that although the rates of reactions with methyl radicals are slowed down by an energetic barrier higher than 30 kcal/mol, those with atomic hydrogen are faster because of the lower activation energy (16.2 kcal/mol). This represents a first clear indication of the relevant effect of the carrier gas in the global kinetics of GaN MOVPE. Concerning reaction 21, it is interesting to notice that it represents an alternative to the condensation pathway to produce the first gallium-nitrogen adducts. Moreover, the reaction has no activation energy because the formation of the new Ga-N bond takes place contemporarily to the cleavage of the Ga-C bond. This reaction is sterically unhindered, because $\text{NH}_2\cdot$ approaches $\text{Ga}(\text{CH}_3)_3$ perpendicular to the Ga-C plane, and the bond formation involves the free Ga 4p_z orbital and the unpaired $\text{NH}_2\cdot$ electron. The same qualitative mechanism is active in reaction 22.

Reactions 21 and 22 proceed significantly faster than reactions 19 and 20 because of the absence of activation energy. In particular, at 1000 °C, the ratio of the rates of reaction 22 with respect to reaction 20 is 2.13×10^4 , which indicates that the dominant reaction route at this temperature consists of the substitution of methyl groups with NH_2 and H.

Summarizing, the calculated rate constants indicate that, in an atmosphere in which $\text{Ga}(\text{CH}_3)_3$, NH_3 , and H_2 are present in significant concentrations, methyl radicals will be generated quickly at temperatures higher than that of the decomposition of $\text{Ga}(\text{CH}_3)_3$ or in the presence of a heated surface on which Ga decomposition can take place. Then methyl radicals will react with NH_3 and H_2 to form $\text{NH}_2\cdot$ and $\text{H}\cdot$ radicals, which in turn will react with $\text{Ga}(\text{CH}_3)_3$ to form $\text{Ga}(\text{CH}_3)_2\text{NH}_2$ and $\text{Ga}(\text{CH}_3)_2\text{H}$. Among the products of these reactions is again $\text{CH}_3\cdot$. Because $\text{CH}_3\cdot$ is consumed and produced in equal amounts in this reaction cycle, we have just described a radical chain mechanism in which methyl radicals catalyze the conversion of $\text{Ga}(\text{CH}_3)_3$ in $\text{Ga}(\text{CH}_3)_2\text{NH}_2$ and $\text{Ga}(\text{CH}_3)_2\text{H}$. Once formed, $\text{Ga}(\text{CH}_3)_2\text{NH}_2$ and $\text{Ga}(\text{CH}_3)_2\text{H}$ are likely to react further with

TABLE 4: Kinetic Constants Involved in the First Catalytic Cycle and Relative Reaction Enthalpies (Calculated at 298 K)^a

	reaction	$\log_{10}A$	α	E_a	ΔH_r
19	$\text{Ga}(\text{CH}_3)_3 + \text{CH}_3 \cdot \rightarrow \text{Ga}(\text{CH}_3)_2 + \text{C}_2\text{H}_6 + \text{CH}_3 \cdot$	8.928	1.0	30.90	12.58
20	$\text{Ga}(\text{CH}_3)_3 + \text{H} \cdot \rightarrow \text{Ga}(\text{CH}_3)_2 + \text{CH}_3 \cdot + \text{CH}_4$	10.330	1.0	16.17	-4.94
21	$\text{Ga}(\text{CH}_3)_3 + \text{NH}_2 \cdot \rightarrow \text{Ga}(\text{CH}_3)_2\text{NH}_2 + \text{CH}_3 \cdot$	12.407	0.5	0.00	-19.10
22	$\text{Ga}(\text{CH}_3)_3 + \text{H} \cdot \rightarrow \text{Ga}(\text{CH}_3)_2\text{H} + \text{CH}_3 \cdot$	12.435	0.5	0.00	-9.41
23	$\text{Ga}(\text{CH}_3)_2\text{NH}_2 + \text{CH}_3 \cdot \rightarrow \text{C}_2\text{H}_6 + \text{Ga}(\text{NH}_2) + \text{CH}_3 \cdot$	8.928	1.0	30.90	7.55
24	$\text{Ga}(\text{CH}_3)_2\text{NH}_2 + \text{H} \cdot \rightarrow \text{Ga}(\text{NH}_2) + \text{CH}_4 + \text{CH}_3 \cdot$	10.760	1.0	16.14	-9.96
25	$\text{Ga}(\text{CH}_3)_2\text{NH}_2 + \text{NH}_2 \cdot \rightarrow \text{Ga}(\text{NH}_2)_2\text{CH}_3 + \text{CH}_3 \cdot$	12.279	0.5	0.00	-14.32
26	$\text{Ga}(\text{NH}_2)_2\text{CH}_3 + \text{NH}_2 \cdot \rightarrow \text{Ga}(\text{NH}_2)_3 + \text{CH}_3 \cdot$	12.471	0.5	0.00	-10.02
27	$\text{Ga}(\text{CH}_3)_3 + \text{NH}_2 \cdot \rightarrow \text{Ga}(\text{NH}_2) + \text{CH}_3 \cdot$	11.592	0.5	0.00	-24.13
28	$\text{Ga}(\text{CH}_3)_2\text{H} + \text{H} \cdot \rightarrow \text{Ga}(\text{CH}_3)_2 + \text{CH}_3 \cdot$	12.259	0.5	0.00	-9.72
29	$\text{Ga}(\text{CH}_3)_2\text{H} + \text{H} \cdot \rightarrow \text{GaH}_3 + \text{CH}_3 \cdot$	11.958	0.5	0.00	-8.28
30	$\text{Ga}(\text{CH}_3)_2\text{H} + \text{NH}_2 \cdot \rightarrow \text{Ga}(\text{CH}_3)\text{NH}_2\text{H} + \text{CH}_3 \cdot$	12.231	0.5	0.00	-19.20
31	$\text{Ga}(\text{CH}_3)\text{NH}_2\text{H} + \text{NH}_2 \cdot \rightarrow \text{Ga}(\text{NH}_2)_2\text{H} + \text{CH}_3 \cdot$	11.929	0.5	0.00	-13.24
32	$\text{Ga}(\text{NH}_2)_2\text{H} + \text{NH}_2 \cdot \rightarrow \text{Ga}(\text{NH}_2)_3 + \text{H} \cdot$	11.857	0.5	0.00	-1.26

^a Reaction rate coefficients expressed as $k = AT^\alpha \exp(-E_a/RT)$; data consistent with units in kcal, mol, cm, s

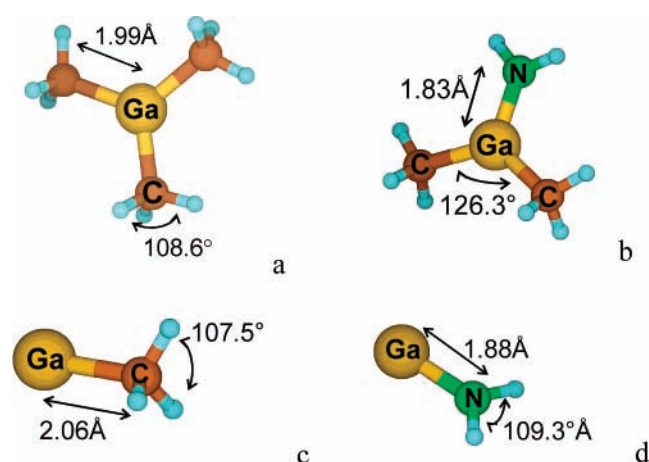


Figure 5. Optimized geometries calculated at the B3LYP/6-311+(d,p) level of theory of (a) TMGa, (b) $\text{Ga}(\text{CH}_3)_2\text{NH}_2$, (c) $\text{Ga}(\text{CH}_3)$, and (d) $\text{Ga}(\text{NH}_2)$.

$\text{CH}_3 \cdot$, $\text{NH}_2 \cdot$, and $\text{H} \cdot$ along the same trend of $\text{Ga}(\text{CH}_3)_3$. The kinetic constants and enthalpy changes of these reactions are reported in Table 4.

The gallium–nitrogen compound $\text{Ga}(\text{CH}_3)_2\text{NH}_2$ produced in reaction 21 can then further react with other radicals to form $\text{Ga}(\text{NH}_2)$ and $\text{Ga}(\text{NH}_2)_2\text{CH}_3$ following the same pathway of $\text{Ga}(\text{CH}_3)_3$.

Reactions 23 and 24 have almost the same activation energy of reactions 19 and 20 and pass through a similar transition state. In particular, reactions that involve a methyl radical have a higher activation energy with respect to those with hydrogen

and are characterized by a lower pre-exponential factor, which can be attributed to the different values of translational partition functions. Similar to $\text{Ga}(\text{CH}_3)_3$ and $\text{Ga}(\text{CH}_3)_2\text{NH}_2$, $\text{Ga}(\text{NH}_2)_2\text{CH}_3$ can also react with $\text{NH}_2 \cdot$ to form $\text{Ga}(\text{NH}_2)_3$. The same reaction of substitution of a methyl group with NH_2 is also active for $\text{Ga}(\text{CH}_3)$.

Finally, we can also observe that gallium hydrates, formed in reactions 22, 28, and 29, can follow the same reaction mechanism of $\text{Ga}(\text{CH}_3)_2\text{NH}_2$. The substitution of CH_3 with H is in fact exothermic by about -10 kcal/mol and proceeds without activation energy. The Ga hydrides so formed can also react with $\text{NH}_2 \cdot$ substituting residual CH_3 and H group with amino groups. The substitution of H with CH_3 is in general exothermic by about -20 kcal/mol, whereas substitution of H with NH_2 is in general athermic.

Some preliminary conclusions can be drawn from the analysis of reactions 19–32. The first is that at temperatures typical of GaN deposition the $\text{Ga}(\text{CH}_3)_3$ precursor dissociates, generating methyl radicals. These radicals react with ammonia and H_2 to form $\text{NH}_2 \cdot$ and $\text{H} \cdot$. Successive reactions will lead to the substitution of $\text{Ga}(\text{CH}_3)$ with $\text{Ga}(\text{NH}_2)$ and $\text{Ga}(\text{H})$. Given the tendency of tricoordinated Ga to dissociate and the stability of the $\text{Ga}-\text{NH}_2$ bond, it is likely that this radical mechanism will lead to the rapid formation of $\text{Ga}(\text{NH}_2)$. We therefore advance the hypothesis that this molecule might represent a key GaN compound both for the gas-phase chemistry and the surface growth chemistry. $\text{Ga}(\text{NH}_2)$, the structure of which is sketched in Figure 5 together with that of other important intermediates, is a particularly stable molecule. In fact, the comparison between the enthalpy changes for reactions 21, 25, and 26, in which an amino substitutes a methyl group in a tricoordinated Ga

TABLE 5: Kinetic Constants and Enthalpy Changes of Nitrogen Radical Formation Reactions^a

	reaction	$\log_{10}A$	α	E_a	ΔH_r
33	$\text{Ga}(\text{NH}_2) + \text{H} \cdot \rightarrow \text{GaNH} \cdot + \text{H}_2$	10.575	1.0	7.83	3.89
34	$\text{Ga}(\text{NH}_2) + \text{NH}_2 \cdot \rightarrow \text{GaNH} \cdot + \text{NH}_3$	10.852	1.0	4.47	4.44
35	$\text{Ga}(\text{NH}_2) + \text{CH}_3 \cdot \rightarrow \text{GaNH} \cdot + \text{CH}_4$	10.716	1.0	11.05	4.67
36	$\text{Ga}(\text{CH}_3)_2\text{NH}_2 + \text{CH}_3 \cdot \rightarrow \text{Ga}(\text{CH}_3)_2\text{NH} \cdot + \text{CH}_4$	10.573	1.0	11.05	5.18
37	$\text{Ga}(\text{CH}_3)_2\text{NH}_2 + \text{H} \cdot \rightarrow \text{Ga}(\text{CH}_3)_2\text{NH} \cdot + \text{H}_2$	11.298	1.0	9.21	4.40
38	$\text{Ga}(\text{CH}_3)_2\text{NH}_2 + \text{NH}_2 \cdot \rightarrow \text{Ga}(\text{CH}_3)_2\text{NH} \cdot + \text{NH}_3$	11.086	1.0	7.69	4.98
39	$\text{Ga}(\text{NH}_2)_2\text{CH}_3 + \text{CH}_3 \cdot \rightarrow \text{Ga}(\text{CH}_3)(\text{NH}_2)\text{NH} \cdot + \text{CH}_4$	10.568	1.0	11.05	3.90
40	$\text{Ga}(\text{NH}_2)_2\text{CH}_3 + \text{H} \cdot \rightarrow \text{Ga}(\text{CH}_3)(\text{NH}_2)\text{NH} \cdot + \text{H}_2$	10.294	1.0	8.72	3.12
41	$\text{Ga}(\text{NH}_2)_2\text{CH}_3 + \text{NH}_2 \cdot \rightarrow \text{Ga}(\text{CH}_3)(\text{NH}_2)\text{NH} \cdot + \text{NH}_3$	10.360	1.0	6.36	3.69
42	$\text{Ga}(\text{NH}_2)_3 + \text{CH}_3 \cdot \rightarrow \text{Ga}(\text{NH}_2)_2\text{NH} \cdot + \text{CH}_4$	10.568	1.0	11.05	2.25
43	$\text{Ga}(\text{NH}_2)_3 + \text{H} \cdot \rightarrow \text{Ga}(\text{NH}_2)_2\text{NH} \cdot + \text{H}_2$	10.575	1.0	7.83	1.47
44	$\text{Ga}(\text{NH}_2)_3 + \text{NH}_2 \cdot \rightarrow \text{Ga}(\text{NH}_2)_2\text{NH} \cdot + \text{NH}_3$	10.340	1.0	4.29	2.05

^a Reaction rate coefficients expressed as $k = AT^\alpha \exp(-E_a/RT)$; data consistent with units in kcal, mol, cm, s. Reaction enthalpies are calculated at 298 K.

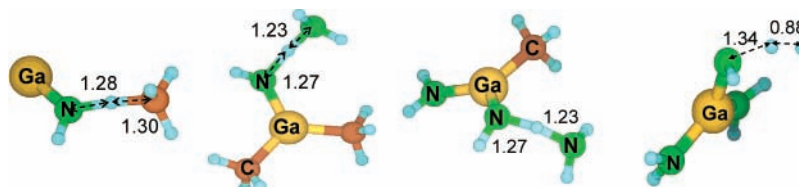


Figure 6. Transition-state structure for reactions 35, 38, 41, and 43. Distances are reported in angstroms.

TABLE 6: Kinetic Constants Determined Adopting Collisional Theory and Expressed as $\text{cm}^3/\text{mol}\cdot\text{s}$

	reaction	$\log_{10}A$
48	$\text{GaNH}\cdot + \text{Ga}(\text{CH}_3) \rightarrow \text{Ga}(\mu 2 - \text{NH})\text{Ga} + \text{CH}_3\cdot$	12.435
49	$\text{GaNH}\cdot + \text{Ga}(\text{CH}_3)_3 \rightarrow \text{Ga}(\mu 2 - \text{NH})\text{Ga}(\text{CH}_3)_2 + \text{CH}_3\cdot$	12.439
50	$\text{GaNH}\cdot + \text{Ga}(\text{CH}_3)_2\text{NH}_2 \rightarrow \text{Ga}(\mu 2 - \text{NH})\text{Ga}(\text{CH}_3)(\text{NH}_2) + \text{CH}_3\cdot$	12.425
51	$\text{GaNH}\cdot + \text{Ga}(\text{NH}_2)_2\text{CH}_3 \rightarrow \text{Ga}(\mu 2 - \text{NH})\text{Ga}(\text{NH}_2)_2 + \text{CH}_3\cdot$	12.438
55	$\text{Ga}(\text{CH}_3)_2\text{NH}\cdot + \text{Ga}(\text{CH}_3)_3 \rightarrow (\text{CH}_3)_2\text{Ga}(\mu 2 - \text{NH})\text{Ga}(\text{CH}_3)_2 + \text{CH}_3\cdot$	12.371
56	$\text{GaCH}_3\text{NH}_2\text{NH}\cdot + \text{Ga}(\text{CH}_3)_3 \rightarrow (\text{CH}_3)(\text{NH}_2)\text{Ga}(\mu 2 - \text{NH})\text{Ga}(\text{CH}_3)_2 + \text{CH}_3\cdot$	12.365
57	$\text{Ga}(\text{NH}_2)_2\text{NH}\cdot + \text{Ga}(\text{CH}_3)_3 \rightarrow (\text{NH}_2)_2\text{Ga}(\mu 2 - \text{NH})\text{Ga}(\text{CH}_3)_2 + \text{CH}_3\cdot$	12.369
58	$\text{Ga}(\text{CH}_3)_2\text{NH}\cdot + \text{Ga}(\text{CH}_3)_2\text{NH}_2 \rightarrow (\text{CH}_3)_2\text{Ga}(\mu 2 - \text{NH})\text{Ga}(\text{CH}_3)(\text{NH}_2) + \text{CH}_3\cdot$	12.369
59	$\text{Ga}(\text{CH}_3)(\text{NH}_2)\text{NH}\cdot + \text{Ga}(\text{CH}_3)_2\text{NH}_2 \rightarrow (\text{CH}_3)(\text{NH}_2)\text{Ga}(\mu 2 - \text{NH})\text{Ga}(\text{CH}_3)(\text{NH}_2) + \text{CH}_3\cdot$	12.367
60	$\text{Ga}(\text{CH}_3)(\text{NH}_2)\text{NH}\cdot + \text{Ga}(\text{CH}_3)_2\text{NH}_2 \rightarrow (\text{CH}_3)(\text{NH}_2)\text{Ga}(\mu 2 - \text{NH})\text{Ga}(\text{CH}_3)(\text{NH}_2) + \text{CH}_3\cdot$	12.367
61	$\text{Ga}(\text{NH}_2)_2\text{NH}\cdot + \text{Ga}(\text{CH}_3)_2\text{NH}_2 \rightarrow (\text{NH}_2)_2\text{Ga}(\mu 2 - \text{NH})\text{Ga}(\text{CH}_3)(\text{NH}_2) + \text{CH}_3\cdot$	12.369
62	$\text{Ga}(\text{CH}_3)_2\text{NH}\cdot + \text{Ga}(\text{NH}_2)_2\text{CH}_3 \rightarrow (\text{CH}_3)_2\text{Ga}(\mu 2 - \text{NH})\text{Ga}(\text{NH}_2)_2 + \text{CH}_3\cdot$	12.367
63	$\text{Ga}(\text{CH}_3)(\text{NH}_2)\text{NH}\cdot + \text{Ga}(\text{NH}_2)_2\text{CH}_3 \rightarrow (\text{CH}_3)(\text{NH}_2)\text{Ga}(\mu 2 - \text{NH})\text{Ga}(\text{NH}_2)_2 + \text{CH}_3\cdot$	12.365
64	$\text{Ga}(\text{NH}_2)_2\text{NH}\cdot + \text{Ga}(\text{NH}_2)_2\text{CH}_3 \rightarrow (\text{NH}_2)_2\text{Ga}(\mu 2 - \text{NH})\text{Ga}(\text{NH}_2)_2 + \text{CH}_3\cdot$	12.369
65	$\text{Ga}(\text{NH}_2)(\text{CH}_3)\text{NH}\cdot + (\text{CH}_3)_2\text{Ga}(\mu 2 - \text{NH})\text{Ga}(\text{CH}_3)_2 \rightarrow (\text{NH}_2)(\text{CH}_3)\text{Ga}(\mu 2 - \text{NH})\text{Ga}(\text{CH}_3)(\mu 2 - \text{NH})\text{Ga}(\text{CH}_3)_2 + \text{CH}_3\cdot$	12.364
66	$\text{Ga}(\text{NH}_2)(\text{CH}_3)\text{NH}\cdot + (\text{CH}_3)_2\text{Ga}(\mu 2 - \text{NH})\text{Ga}(\text{NH}_2)_2 \rightarrow (\text{NH}_2)(\text{CH}_3)\text{Ga}(\mu 2 - \text{NH})\text{Ga}(\text{CH}_3)(\mu 2 - \text{NH})\text{Ga}(\text{NH}_2)_2 + \text{CH}_3\cdot$	12.363
67	$\text{Ga}(\text{CH}_3)_2\text{NH}\cdot + (\text{CH}_3)_2\text{Ga}(\mu 2 - \text{NH})\text{Ga}(\text{NH}_2)_2 \rightarrow (\text{NH}_2)_2\text{Ga}(\mu 2 - \text{NH})\text{Ga}(\text{CH}_3)(\mu 2 - \text{NH})\text{Ga}(\text{CH}_3)_2 + \text{CH}_3\cdot$	12.361
68	$\text{Ga}(\text{CH}_3)_2\text{NH}\cdot + (\text{CH}_3)(\text{NH}_2)\text{Ga}(\mu 2 - \text{NH})\text{Ga}(\text{NH}_2)_2 \rightarrow (\text{NH}_2)\text{Ga}(\mu 2 - \text{NH})\text{Ga}(\text{NH}_2)(\mu 2 - \text{NH})\text{Ga}(\text{CH}_3)_2 + \text{CH}_3\cdot$	12.355

compound, with that of reactions 27, which involves a mono-coordinated Ga molecule, shows that the Ga–NH₂ bond in the monocoordinated molecule is more stable by 5–10 kcal/mol than in the tricoordinated Ga compound. The major stability of GaNH₂ can be ascribed to its peculiar electronic conformation, which has an electron doublet over both the gallium and nitrogen atoms; upon binding, the nitrogen electron doublet can interact with the empty d orbitals of gallium, increasing the bond energy between the two atoms with respect to the tricoordinated Ga complex. In fact, the enthalpy changes of reactions 21, 25, and 26 decrease from –19.1 to –14.3, and to –10.0 kcal/mol with the progressive substitution of CH₃ with NH₂ groups. This corresponds to an increase of the Mulliken charges of the gallium atom from 0.69 to 0.76 and to 0.85. We can thus conclude that the decrease of the Ga–NH₂ bond energy with the degree of NH₂/CH₃ substitution is determined by the electrophilicity of NH₂.

The kinetic mechanism summarized in Tables 3 and 4 provides a fast route for the formation of GaN adducts containing one gallium atom and different amino groups (from one to three) and reactive radicals: CH₃·, H·, and NH₂·. All of these molecules can then react together, increasing the number and size of GaN gas-phase species. Because of the higher stability of nitrogen radicals with respect to gallium, the next reactive steps we decided to study were the attack of the CH₃·, H·, and NH₂· radicals to the first generation of Ga species to form Ga–amino radicals. The reactions investigated are reported in Table 5 along with pre-exponential factors, activation energies, and enthalpy changes, while the transition-state structures of some representative reactions are sketched in Figure 6. These reactions are characterized by an activation energy smaller than that of the reactions of formation of the initial methyl radicals and thus proceed quickly, leading to the production of a large amounts of new nitrogen radicals.

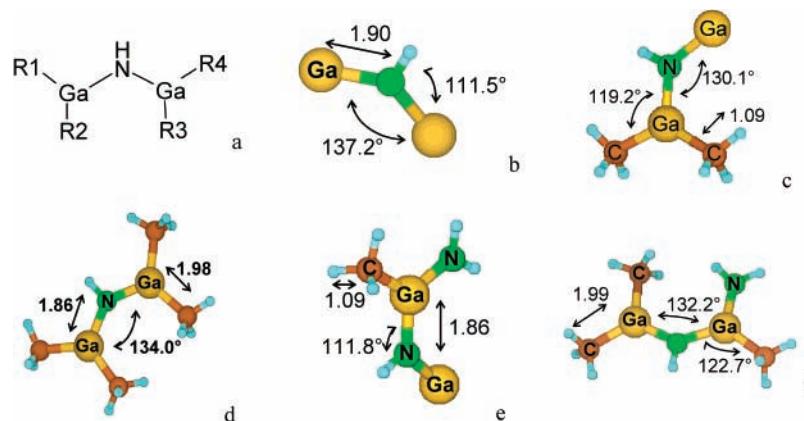


Figure 7. (a) Structure of adducts produced through the second catalytic cycle: R1, R2, R3, and R4 represent CH₃, NH₂, H, or a vacancy. Optimized geometry of (b) GaNHGa, (c) (CH₃)₂Ga(μ2 – NH)Ga, (d) (CH₃)₂Ga(μ2 – NH)Ga(CH₃)₂, (e) Ga(μ2 – NH)Ga, and (f) (CH₃)(NH₂)Ga(CH₃)₂(μ2 – NH)Ga(CH₃)(NH₂). Distances are reported in angstroms, and angles are reported in degrees.

TABLE 7: Kinetic Constants of Reactions Leading to the Formation of Nitrogen Radicals^a

	reaction	$\log_{10}A$	α	E_a
69	$(\text{CH}_3)_2\text{Ga}(\mu 2 - \text{NH})\text{Ga}(\text{CH}_3)(\text{NH}_2) + \text{CH}_3^\bullet \rightarrow (\text{CH}_3)_2\text{Ga}(\mu 2 - \text{NH})\text{Ga}(\text{CH}_3)\text{NH}^\bullet + \text{CH}_4$	10.591	1.0	11.05
70	$(\text{CH}_3)_2\text{Ga}(\mu 2 - \text{NH})\text{Ga}(\text{CH}_3)(\text{NH}_2) + \text{NH}_2^\bullet \rightarrow (\text{CH}_3)_2\text{Ga}(\mu 2 - \text{NH})\text{Ga}(\text{CH}_3)\text{NH}^\bullet + \text{NH}_3$	10.340	1.0	5.00
71	$(\text{NH}_2)(\text{CH}_3)\text{Ga}(\mu 2 - \text{NH})\text{Ga}(\text{CH}_3)(\text{NH}_2) + \text{H}^\bullet \rightarrow (\text{NH}_2)(\text{CH}_3)\text{Ga}(\mu 2 - \text{NH})\text{Ga}(\text{CH}_3)\text{NH}^\bullet + \text{H}_2$	10.575	1.0	8.00

^a Reaction rate coefficients expressed as $k = AT^\alpha \exp(-E_a/RT)$; data consistent with units in kcal, mol, cm, s.

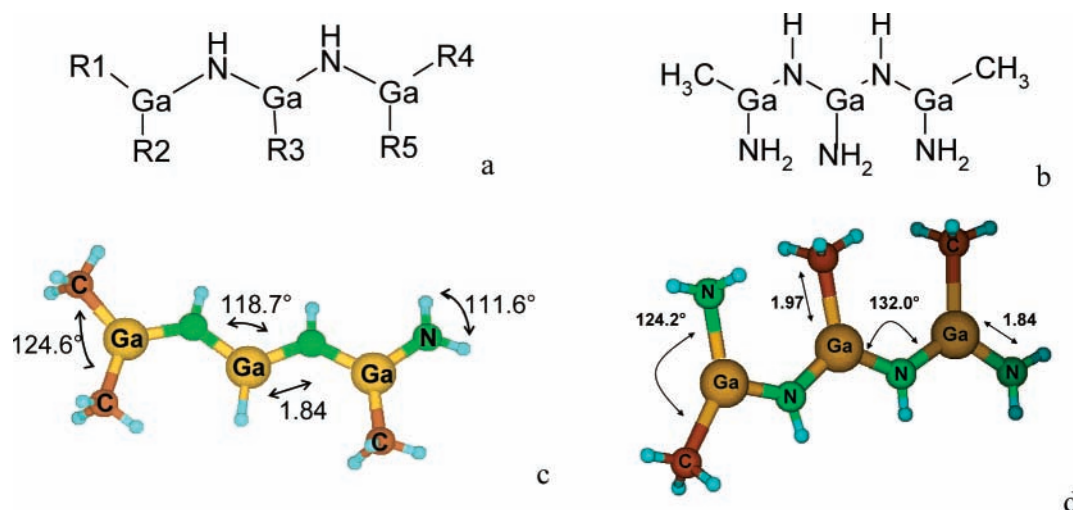


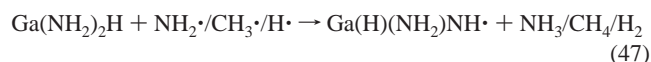
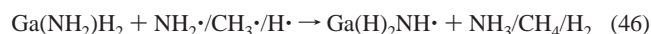
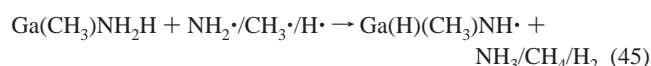
Figure 8. (a) General structure of adducts produced through the third catalytic cycle: R1, R2, R3, R4, and R5 represent CH₃, NH₂, H, or an empty vacancy. Optimized geometry of (b) (CH₃)(NH₂)Ga($\mu 2 - \text{NH}$)Ga(NH₂) ($\mu 2 - \text{NH}$) Ga(CH₃)(NH₂), (c) (CH₃)₂Ga($\mu 2 - \text{NH}$)Ga(CH₃) ($\mu 2 - \text{NH}$) Ga(CH₃)(NH₂), and (d) (CH₃)(NH₂)Ga($\mu 2 - \text{NH}$)Ga(CH₃) ($\mu 2 - \text{NH}$) Ga(CH₃)(NH₂). Distances are reported in angstroms, and angles are reported in degrees.

TABLE 8: Kinetic Constants and Enthalpy Changes of Intramolecular Condensation Reactions That Produce Cyclic Compounds^a

	reaction	$\log_{10}A$	α	E_a	ΔH_f
72	$(\text{CH}_3)_2\text{Ga}(\mu 2 - \text{NH})\text{Ga}(\text{CH}_3)(\mu 2 - \text{NH})\text{Ga}(\text{CH}_3)(\text{NH}_2) \rightarrow [\text{CH}_3\text{GaNH}]_3 + \text{CH}_4$	9.041	1.0	24.0	-17.70
73	$(\text{CH}_3)(\text{H})\text{Ga}(\mu 2 - \text{NH})\text{Ga}(\text{H})(\mu 2 - \text{NH})\text{Ga}(\text{H})(\text{NH}_2) \rightarrow [\text{HGaNH}]_3 + \text{CH}_4$	10.330	1.0	16.7	-6.32

^a Reaction rate coefficients expressed as $k = A \cdot T^\alpha \exp(-E_a/RT)$; data consistent with units in kcal, mol, cm, s. Reaction enthalpies are calculated at 298 K.

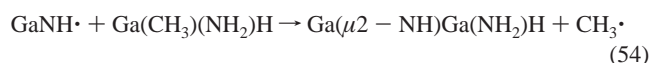
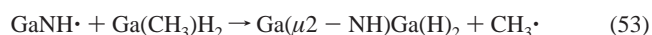
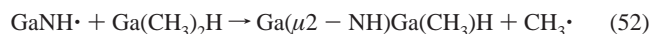
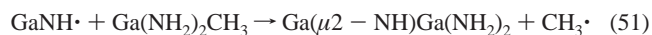
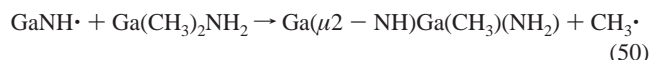
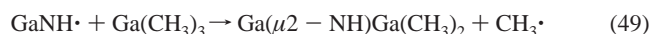
In addition to the reactions reported in Table 5, we determined kinetic constants for similar reactions involving hydrogenated species: Ga(CH₃)NH₂H, Ga(NH₂)₂H₂, and Ga(NH₂)₂H.



We found that these kinetic steps have almost the same activation energy as those characterized by the presence of a methyl group in spite of H.

3.3.2. Second Catalytic Cycle. The production of Ga amino radicals implies the formation of a new generation of radicals, which can then start a second catalytic cycle, whose products will be larger GaN gas-phase compounds. In this section, we report kinetic constants calculated for reactions between nitrogen radicals produced in the first catalytic cycle and all of the reactive neutral species present in the gas phase. In particular, similar to what was found previously, we calculated that reactions involving the abstraction of hydrogen atoms bonded to a nitrogen or a carbon atom are hindered by a high activation energy. On the contrary, we studied the possibility of a radical-exchange reaction that proceeds through the formation of a bond

between the nitrogen of a radical molecule and the gallium of a neutral adduct, produced as a result of the first catalytic cycle, followed by the consequent elimination of a methyl radical. The elimination of a methyl group from the formed adduct is due to the instability of a compound in which gallium has valence 2, as mentioned already.



Here we have reported for the sake of brevity only the reactions (48–54) between the GaNH[•] radical and the Ga gas-phase species generated in the first cycle. The same reactions have, however, been investigated for the following radicals: Ga(CH₃)₂NH[•], Ga(CH₃)(NH₂)NH[•], and Ga(NH₂)₂NH[•]. These reactions are characterized by the formation of different GaN

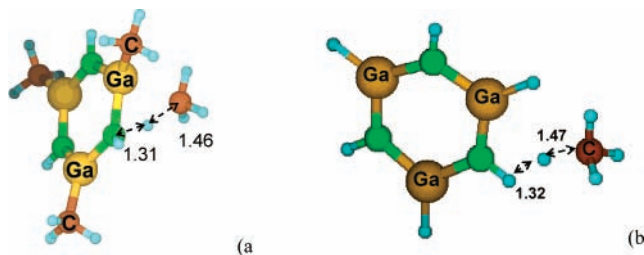


Figure 9. Transition-state structure for reactions (a) 73 and (b) 74. Distances are reported in angstroms.

gas-phase compounds composed of a linear sequence of 3, 4, and 5 gallium or nitrogen atoms and by the production of methyl radicals that close the radical chain. Because these reactions do not present an activation energy, their kinetic constants were determined with collisional theory. Collisional kinetic constants determined for some of these reactions are reported in Table 6 and, because it is possible to observe, are similar (reactions involving Ga hydrides have been omitted). The general structure of all 55 possible adducts formed through the second catalytic

cycle along with the geometry of five representative molecules is reported in Figure 7.

After being generated, these large GaN adducts can then react, following the same pathway proposed for the first catalytic cycle, with all of the radical species present in the gas phase to form new nitrogen radicals. Of course, the number of reactions is increased with respect to those investigated for the first catalytic cycle, but their rate constants are similar and, in particular, the kinetic parameters are not influenced by the kind of radical but only by the chemical composition of the neutral reactant. As in the case of the first catalytic cycle, the calculated activation energies are between 5 and 12 kcal/mol, as can be observed in Table 7, where three representative nitrogen radical formation reactions are reported.

It is interesting to observe that, summing the reactions in Table 7 in which a methyl radical is consumed, to those in Table 6 in which a methyl radical is produced, it is possible to obtain a catalytic mechanism by which small GaN adducts are converted to large GaN species and radicals are neither produced nor consumed. The rate of this mechanism is particularly high, given the fact that the reactions involved require overcoming

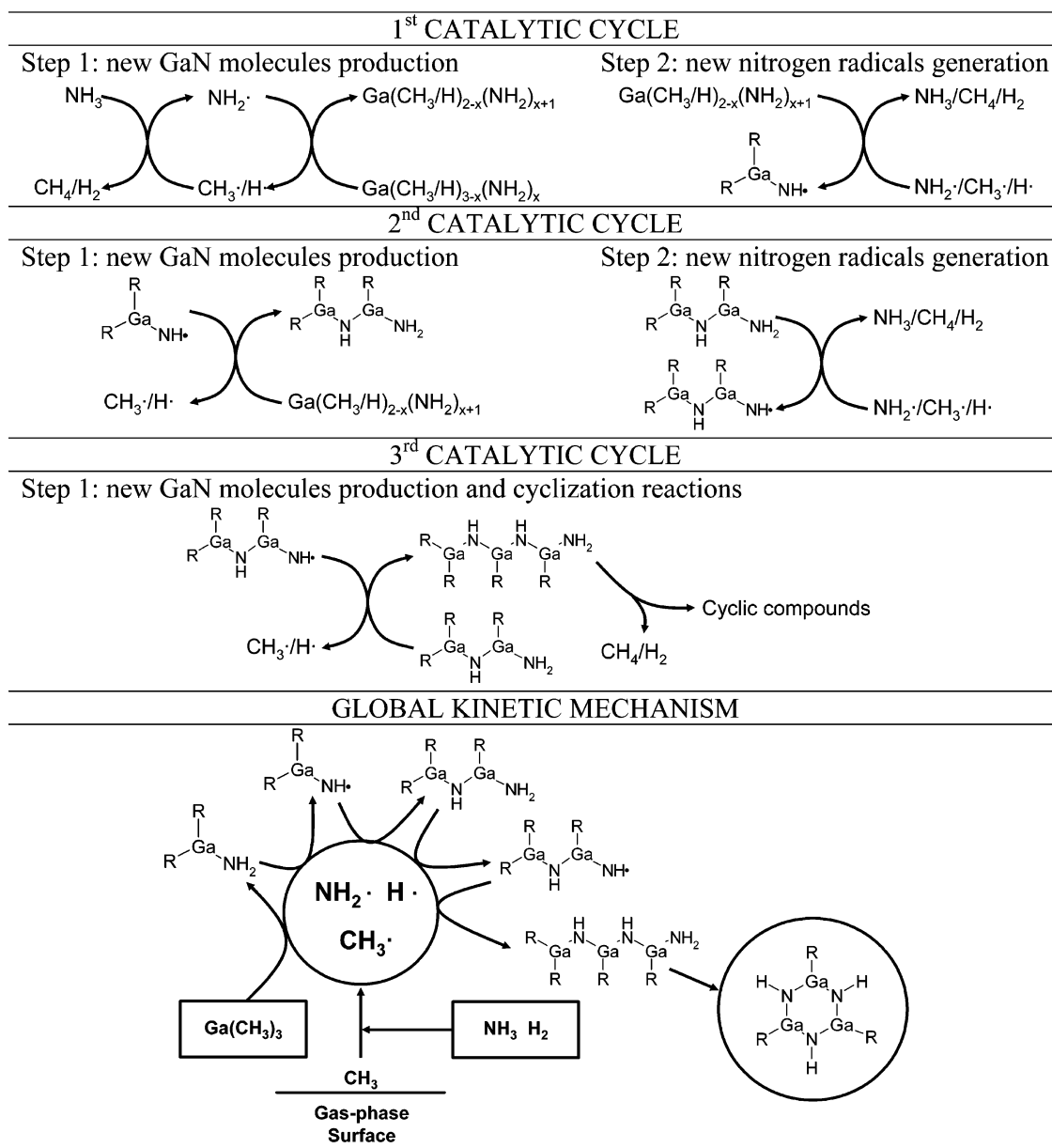


Figure 10. Graphical representation of the catalytic cycles involved in the radical chain mechanism.

activation energies similar to those reported in Table 7, with values smaller than 12 kcal/mol.

3.3.3. Third Catalytic Cycle and Cyclization Reactions. Following the same reactive steps of the second catalytic cycle, the global kinetic mechanism was incremented with reactions involving molecules produced in the second catalytic cycle. In particular, we determined the rate constants of all of the reactions between the second-generation nitrogen radical and all of the neutral species produced in the first catalytic cycle. The same radical-exchange reaction mechanism described in the previous paragraph leads to the production of GaN gas-phase adducts formed by gallium and nitrogen atoms in a number between 5 and 7. In Figure 8 are reported the global adduct structures of the GaN compounds that can be produced through the third step of the catalytic cycle. The chemical composition of these compounds is characterized by a sequence of three gallium atoms bonded by two $-NH-$ groups. Obviously, the number of possible adducts is increased enormously with respect to those produced during the second catalytic cycle because there are five different residues, R, which can be a vacancy, a hydrogen, a methyl, or an amino group.

Summarizing, the global kinetic scheme developed is composed of a series of fast radical chain reactions that lead to the formation of gas-phase compounds composed of gallium and nitrogen atoms, which go from the simple $Ga(NH_2)$ molecule to more complicated and larger molecules characterized by the presence of three gallium atoms and up to six NH_x groups. This kinetic mechanism could be complicated easily considering successive catalytic cycles that bring the formation of increasingly larger adducts. However, the aim of this computational investigation is not necessarily to describe the formation of large GaN adducts but rather to demonstrate that a radical mechanism can lead to the formation of thermodynamically stable GaN gas-phase species. We therefore limited our study to the formation of species comprising three Ga atoms because we have shown previously that a cyclic Ga_3N_3 chemical species is thermodynamically favored in the investigated conditions.

These species can be produced from linear adducts through an intramolecular condensation reaction (reported in Table 8) whose products are methane and a cyclic compound. Reactions 72 and 73 differ for the nature of the Ga substituents (H or CH_3). The kinetic constants of these reactions were computed with transition-state theory and were found to have a distinct transition state. The calculated activation energies for the formation of cyclic compounds are between the values determined for reactions 72 and 73, which are 24.0 and 16.7 kcal/mol, respectively. Although reactions 72 and 73 have relatively high activation energies compared to those computed for radical reactions, they proceed quickly during the GaN MOVPE because they are unimolecular reactions, and their reaction half-life time, $t^{1/2}$ (6.5 ns), is much smaller than the typical residence time in MOVPE reactors. In Figure 9, we report the transition-state structures of these reactions, and Arrhenius parameters are shown in Table 8.

The three catalytic cycles and the global kinetic mechanism are shown in Figure 10.

Conclusions

On the basis of our investigation, we can draw the following conclusions:

(1) A gas-phase atmosphere in which $Ga(CH_3)_3$ is diluted in ammonia and H_2 will react quickly through a radical chain mechanism when the $Ga(CH_3)_3$ decomposition temperature is reached.

(2) The reactions will proceed about 2 orders of magnitude faster if H_2 is present in a significant concentration because it promotes the formation of $H\cdot$ and $NH_2\cdot$ radicals. This is confirmed by experimental evidence according to which the nucleation of GaN powders is suppressed if H_2 is not present in the gas phase.^{7,9} This is in agreement with fluid dynamic simulations we performed using a lumped version of the mechanism presented here,⁵³ which showed that removing H_2 from the inlet mixture reduces the predicted GaN nuclei concentration by 2 orders of magnitude.

(3) Our mechanism suggests that $Ga(NH_2)$ is among the main product of the radical chain mechanism. Because its concentration is dependent on that of H_2 , and experimental studies have shown that GaN deposition rate can be increased by adding hydrogen to the mixture,^{54,55} we advance the hypothesis that it is a key precursor to film growth.

(4) The main product of this investigation is a detailed chemical mechanism, comprising more than 200 species involved in more than 400 reactions. We believe that its insertion in a suitable fluid dynamic model will help to identify the key MOVPE parameters, such as reactor geometry and operating conditions, which operate in order to decrease the gas-phase powder formation and improve the quality of the deposited films.

Supporting Information Available: Thermodynamic parameters of key chemical species. This material is available free of charge via the Internet at <http://pubs.acs.org>.

References and Notes

- (1) Jones, A. C.; O'Brien, P. *CVD of Compound Semiconductors*; VHC: Weinheim, Germany, 1997.
- (2) Nakamura, S.; Fasol, G. *The Blue Laser Diode*; Springer: Berlin, 1997.
- (3) Trew, R. J. P. *IEEE* **2002**, *90*, 1032.
- (4) Timoshkin, A. Y.; Bettinger, H. F.; Schaefer, H. F. *J. Phys. Chem. A* **2001**, *105*, 3249.
- (5) Stringfellow, G. B. *Organometallic Vapor-Phase Epitaxy: Theory and Practice*, 2nd ed.; Academic Press: New York, 1999.
- (6) Schmid, R.; Basting, D. *J. Phys. Chem. A* **2005**, *109*, 2623.
- (7) Creighton, J. R.; Wang, G. T.; Breiland, W. G.; Coltrin, M. E. *J. Cryst. Growth* **2004**, *261*, 204.
- (8) Creighton, J. R.; Wang, G. T. *J. Phys. Chem. A* **2005**, *109*, 10554.
- (9) Creighton, J. R.; Breiland, W. G.; Coltrin, M. E.; Pawlowski, R. *P. Appl. Phys. Lett.* **2002**, *81*, 2626.
- (10) Mihopoulos, T. G.; Gupta, V.; Jensen, K. F. *J. Cryst. Growth* **1998**, *195*, 733.
- (11) Parikh, R. P.; Adomaitis, R. A.; Aumer, M. E.; Partlow, D. P.; Thomson, D. B.; Rubloff, G. W. *J. Cryst. Growth* **2006**, *296*, 15.
- (12) Bergmann, U.; Reimer, V.; Atakan, B. *Phys. Chem. Chem. Phys.* **1999**, *1*, 5593.
- (13) Timoshkin, A. Y.; Suvorov, A. V.; Bettinger, H. F.; Schaefer, H. F. *J. Am. Chem. Soc.* **1999**, *121*, 5687.
- (14) Timoshkin, A. Y.; Schaefer, H. F. *J. Am. Chem. Soc.* **2003**, *125*, 9998.
- (15) Thon, A.; Kuech, T. F. *Appl. Phys. Lett.* **1996**, *69*, 55.
- (16) Sengupta, D. *J. Phys. Chem. B* **2003**, *107*, 291.
- (17) Wang, G. T.; Creighton, J. R. *J. Phys. Chem. A* **2006**, *110*, 1094.
- (18) Kakanakova-Georgieva, A.; Gueorguiev, G. K.; Stafstrom, S.; Hultman, L.; Janzen, E. *Chem. Phys. Lett.* **2006**, *431*, 346.
- (19) Jacko, M. G.; Price, S. J. W. *Can. J. Chem.* **1963**, *41*, 1560.
- (20) Simka, H.; Willis, B. G.; Lengyel, I.; Jensen, K. F. *Prog. Cryst. Growth Charact.* **1997**, *35*, 117.
- (21) Bockhorn, H. *Soot Formation in Combustion: Mechanism and Models*; Springer-Verlag: Berlin, 1994.
- (22) Fascella, S.; Cavallotti, C.; Rota, R.; Carrà, S. *J. Phys. Chem. A* **2005**, *109*, 7546.
- (23) Fascella, S.; Cavallotti, C.; Rota, R.; Carrà, S. *J. Phys. Chem. A* **2004**, *108*, 3829.
- (24) Cavallotti, C.; Bertani, V.; Masi, M.; Carrà, S. *J. Electrochem. Soc.* **1999**, *146*, 3277.

- (25) Cavallotti, C.; Masi, M.; Lovergine, N.; Prete, P.; Mancini, A. M.; Carrà, S. *J. Phys. Chem. A* **1999**, *103*, 411.
- (26) Cavallotti, C.; Nemirovskaya, M.; Jensen, K. F. *J. Cryst. Growth* **2003**, *248*, 411.
- (27) Masi, M.; Cavallotti, C.; Radaelli, G.; Carrà, S. *Cryst. Res. Technol.* **1997**, *32*, 1125.
- (28) Cavallotti, C.; Moscatelli, D.; Masi, M.; Carra, S. *J. Cryst. Growth* **2004**, *266*, 363.
- (29) Cavallotti, C.; Moscatelli, D.; Carra, S. *J. Phys. Chem. A* **2004**, *108*, 1214.
- (30) Moscatelli, D.; Cavallotti, C.; Masi, M.; Carra, S. *J. Cryst. Growth* **2003**, *248*, 31.
- (31) Becke, A. D. *J. Chem. Phys.* **1993**, *98*, 5648.
- (32) Lee, C.; Yang, W.; Parr, R. G. *Phys. Rev. B* **1988**, *37*, 785.
- (33) Dunning, T. H.; Hay, P. J. In *Modern Theoretical Chemistry*; Schaefer, H. F., Ed.; Plenum: New York, 1976; p 1.
- (34) Peng, C.; Schlegel, H. B. *Isr. J. Chem.* **1994**, *33*, 449.
- (35) Peng, C.; Ayala, P. Y.; Schlegel, H. B.; Frisch, M. J. *J. Comput. Chem.* **1996**, *17*, 49.
- (36) Cavallotti, C.; Lengyel, I.; Nemirovskaya, M.; Jensen, K. F. *J. Cryst. Growth* **2004**, *268*, 76.
- (37) Frisch, M. J.; Trucks, G. W.; Schlegel, H. B.; Scuseria, G. E.; Robb, M. A.; Cheeseman, J. R.; Montgomery, J. A., Jr.; Vreven, T.; Kudin, K. N.; Burant, J. C.; Millam, J. M.; Iyengar, S. S.; Tomasi, J.; Barone, V.; Mennucci, B.; Cossi, M.; Scalmani, G.; Rega, N.; Petersson, G. A.; Nakatsuji, H.; Hada, M.; Ehara, M.; Toyota, K.; Fukuda, R.; Hasegawa, J.; Ishida, M.; Nakajima, T.; Honda, Y.; Kitao, O.; Nakai, H.; Klene, M.; Li, X.; Knox, J. E.; Hratchian, H. P.; Cross, J. B.; Bakken, V.; Adamo, C.; Jaramillo, J.; Gomperts, R.; Stratmann, R. E.; Yazyev, O.; Austin, A. J.; Cammi, R.; Pomelli, C.; Ochterski, J. W.; Ayala, P. Y.; Morokuma, K.; Voth, G. A.; Salvador, P.; Dannenberg, J. J.; Zakrzewski, V. G.; Dapprich, S.; Daniels, A. D.; Strain, M. C.; Farkas, O.; Malick, D. K.; Rabuck, A. D.; Raghavachari, K.; Foresman, J. B.; Ortiz, J. V.; Cui, Q.; Baboul, A. G.; Clifford, S.; Cioslowski, J.; Stefanov, B. B.; Liu, G.; Liashenko, A.; Piskorz, P.; Komaromi, I.; Martin, R. L.; Fox, D. J.; Keith, T.; Al-Laham, M. A.; Peng, C. Y.; Nanayakkara, A.; Challacombe, M.; Gill, P. M. W.; Johnson, B.; Chen, W.; Wong, M. W.; Gonzalez, C.; Pople, J. A. *Gaussian 03*, revision C.02; Gaussian, Inc.: Wallingford, CT, 2004.
- (38) Schaftenaar, G.; Noordik, J. H. *J. Comput.-Aided Mol. Des.* **2000**, *14*, 123.
- (39) Granata, S.; Faravelli, T.; Ranzi, E. *Combust. Flame* **2003**, *132*, 533.
- (40) Hardtdegen, H.; Kaluza, N.; Steins, R.; Schmidt, R.; Wirtz, K.; Yakovlev, E. V.; Talalaev, R. A.; Makarov, Y. N. *J. Cryst. Growth* **2004**, *272*, 407.
- (41) Mihopoulos, T. G.; Hummel, S. G.; Jensen, K. F. *J. Cryst. Growth* **1998**, *195*, 725.
- (42) McCaulley, J. A.; McCrary, V. R.; Donnelly, V. M. *J. Phys. Chem.* **1989**, *93*, 1148.
- (43) Donnelly, V. M.; McCaulley, J. A. *Surf. Sci.* **1990**, *238*, 34.
- (44) Francis, J. T.; Benson, S. W.; Tsotsis, T. T. *J. Phys. Chem.* **1991**, *95*, 4583.
- (45) McCaulley, J. A.; Shul, R. J.; Donnelly, V. M. *J. Vac. Sci. Technol., A* **1991**, *9*, 2872.
- (46) Narmann, A.; Yu, M. L. *Surf. Sci.* **1992**, *270*, 1041.
- (47) McDaniel, A. H.; Allendorf, M. D. *Chem. Mater.* **2000**, *12*, 450.
- (48) Yu, Y. X.; Li, S. M.; Xu, Z. F.; Li, Z. S.; Sun, C. C. *Chem. Phys. Lett.* **1998**, *296*, 131.
- (49) Mebel, A. M.; Lin, M. C. *J. Phys. Chem. A* **1999**, *103*, 2088.
- (50) Bryukov, M. G.; Slagle, I. R.; Knyazev, V. D. *J. Phys. Chem. A* **2001**, *105*, 3107.
- (51) Sutherland, J. W.; Su, M. C.; Michael, J. V. *Int. J. Chem. Kinet.* **2001**, *33*, 669.
- (52) Corchado, J. C.; EspinosaGarcia, J. *J. Chem. Phys.* **1997**, *106*, 4013.
- (53) Moscatelli, D.; Caccioppoli, P.; Cavallotti, C. *Appl. Phys. Lett.* **2005**, *86*.
- (54) Richter, E.; Hennig, C.; Weyers, M.; Habel, F.; Tsay, J. D.; Liu, W. Y.; Bruckner, P.; Scholz, F.; Makarov, Y.; Segal, A.; Kaeppler, J. *J. Cryst. Growth* **2005**, *277*, 6.
- (55) Losurdo, M.; Capezzuto, P.; Bruno, G.; Namkoong, G.; Doolittle, W. A.; Brown, A. S. *Phys. Status Solidi A* **2002**, *190*, 43.